INTERNATIONAL JOURNAL of SMART GRID
Buccella C., Cimoroni M.G., Cecati C., Vol.3, No.1, March, 2019

Low-Frequency Harmonic Elimination Technique in Three Phase Cascaded H-Bridges Multilevel Inverters for Renewable Energy Applications

Concettina Buccella, Maria Gabriella Cimoroni, Carlo Cecati

University of L'Aquila - DISIM & DigiPower srl, 67100 L'Aquila, Italy
(concettina.buccella@univaq.it, mariagabriella.cimoroni@univaq.it, carlo.cecati@univaq.it)

Received: 08.02.2019 Accepted: 24.03.2019

Abstract- This paper proposes a selective harmonic elimination technique for medium and high power three phase cascaded H-bridges l-level inverters at fundamental frequency. Compared to other SHE methods, it is capable to delete more harmonics from the output voltage waveform and to provide lower total harmonic distortion values. A mathematical proof is given to demostrate that undeleted harmonics are only those of order $n = 2k(l + r) \pm 1,\ k = 1, 2, \ldots$, where r is an integer parameter that assumes the values $-2, -1, 0$, defining three different sets of switching angles, provided within the whole range of modulation index. Proposed method assumes the availability of different dc voltage sources and pulses patterns, defined for the three sets of switching angles. Simulated results are shown to confirm the validity of the proposed procedure. For $l = 5$ and $l = 7$, obtained results have been compared with those obtained with a conventional SHE technique at the same conditions. Very good performances, in terms of number of deleted harmonics and THD, are observed when $r = 0$, moreover, in comparison with classical SHE, proposed method offers reduced computational complexity because it does not require the solution of non linear equations.

Keywords- Selective Harmonic Elimination, Cascaded H-bridges, Multilevel Inverters, Total Harmonic Distortion, Renewable Energy Systems.

Nomenclature

m	modulation index
α_i	ith switching angle
V_{dci}	ith dc voltage feeding H-bridge
l	inverter levels
s	number of switching angles, $s = \frac{l-1}{2}$
RSS	reference sinusoidal signal
V_m	peak value, in p.u., of *RSS*
ω	angular velocity
$v_{AN}(\omega t)$	output phase voltage
r	integer parameter that assumes the values $-2, -1, 0$

1. Introduction

The integration of distributed generation (DG) systems based on renewable energy resources (e.g., wind turbines, photovoltaic, fuel-cells, biomass, micro-turbines, small hydroelectric plants, and so on) with a distribution grid represents represents the most promising solution to the increasing demand of clean energy, but at the same time it an important issue from technical, economical and environmental points of view [1, 2, 3]. In medium-voltage and high-power systems, multilevel inverters (MLI) represent a good choice in terms of performance and cost [4, 5, 6]. Their best characteristics are: reduced voltage ratings for the adopted power devices, good harmonic spectrum, thus making possible the use of smaller and less expensive filters, and good dynamic response. Technical challenges are focused on increasing inverter's efficiency, improving power quality by reducing THD, decreasing conduction as well as switching losses [7, 8].

In MLI operating with modulations at high frequency, such as phase shifted modulation, switching losses (SL) are significantly higher than conduction losses (CL) as they depend on the number of switching states, therefore, in order to increase overall efficiency, a reduction of switching frequency is necessary [9, 10].

The typical cascaded H-bridge (CHB) multilevel inverter topology requires a high number of switches and related gate drivers, which may lead to an expensive and complex overall system. Therefore, several new multilevel inverter topologies using a reduced number of switches and related gate drivers were developed in recent years [11, 12, 13]. Starting from several levels with equal or unequal dc voltages, MLI produce a stepped waveform from which a sinusoidal waveform is extracted through passive output filter. However, the staircase waveform produced by the MLI contains sharp transitions that result, by Fourier series theory, in harmonics added to the fundamental frequency sinusoidal component [14].

In a typical conversion system for renewable energy, dc power sources of a multilevel inverter are supplied by the renewable energy generators e.g. photovoltaic strings or wind generator that presents fluctuations due to environmental factors. For instance, the outputs of solar cells change due to variations of light intensity, temperature, and so on, wind generation depends of wind characteristics, and so on. Therefore, while control algorithms extract the maximum achievable power, a suitable modulation technique is necessary to convert input energy in the form required by AC distribution line. Many modulation techniques have already been developed for MLI such as those derived by Sinusoidal Pulse Width Modulation (SPWM) such as Phase Shifted PWM (PS-PWM), Space Vector Modulation (SVM) [15, 16, 17, 18], Analytical Selective Harmonic Elimination [19, 20]. Some of them are nonlinear methods, such as hysteresis control [21, 22], sliding mode control [23] and others [24, 25]. In classical SHE approach, the switching angles are the unknowns of the problem [26].

A transcendental equation system that sets to zero the amplitudes of the harmonics to delete, is solved. In order to increase the number of harmonics to be deleted without increasing switching frequency, also the dc voltage levels can be considered as unknowns, thus increasing the number of equations [27, 28, 29, 30].

In [31] a universal formulation, which can be utilized with half-wave symmetry, that provides a unique system of equations valid for any possible multilevel waveform, has been proposed. Thereby, without using predefined waveforms, this formulation provides the ability to search simultaneously both the firing angles and the switching patterns, simplifying significantly the search process and providing a high number of solutions.

In [32] an inclusive comparison of different modulation techniques has been conducted in terms of low-order harmonic elimination and weighted total harmonic distortion (WTHD) by using metaheuristic techniques that have shown remarkable performance in a vast variety of engineering problems.

In [33] a two-stage algorithm has been proposed to compute switching angles for SHE or selective harmonic control. Compared to the traditional numerical methods, the executing efficiency is increased siginificantly.

Paper [34] presents two optimisation techniques, namely backtracking search algorithm and differential search algorithm (DSA) for obtaining a more accurate solution of the harmonics elimination problem. The superiority of the proposed optimisation algorithms over the well known algorithms such as genetic, BEE and particle swarm optimisation has been established by a comparative study with respect to the possibility of getting global minima, the rank of convergence rate, and inverter performance analysis.

In this paper a fundamental frequency SHE technique for three phase CHB l-level inverters is proposed that eliminates a significant number of harmonics from the output voltage, returning high quality waveform. A mathematical proof is included to demonstrate that the undeleted harmonics are only those of order $n = 2k(l+r) \pm 1,\ k = 1, 2, \ldots,$ where r assumes the values $-2, -1, 0$, defining three different sets of equispaced switching angles in the whole range of m. Unequal dc voltage sources, depending on the switching angles, feed the H-bridges. Results are obtained by simulations, confirming the accuracy of the proposed procedure that deletes a higher number of harmonics and returns lower THD respect to the classical SHE method. THD doesn't depend on m and it is shown that the smallest THD is obtained when $r = 0$, except for $l = 9,\ 15,\ 21,\ 27$ where $r = -1$ represents the best choice. Considering three phase CHB 5- and 7- levels inverters, the results obtained by the proposed technique and by the classical SHE [20, 35] at the same conditions, are shown. For all the considered values of m, proposed method with $r = 0$, deletes a higher number of harmonics and provides lower THD, than the considered classical SHE. Moreover proposed method doesn't have to solve non linear equations to find the switching angles, therefore, computational load is much lower than with conventional SHE.

2. Proposed procedure

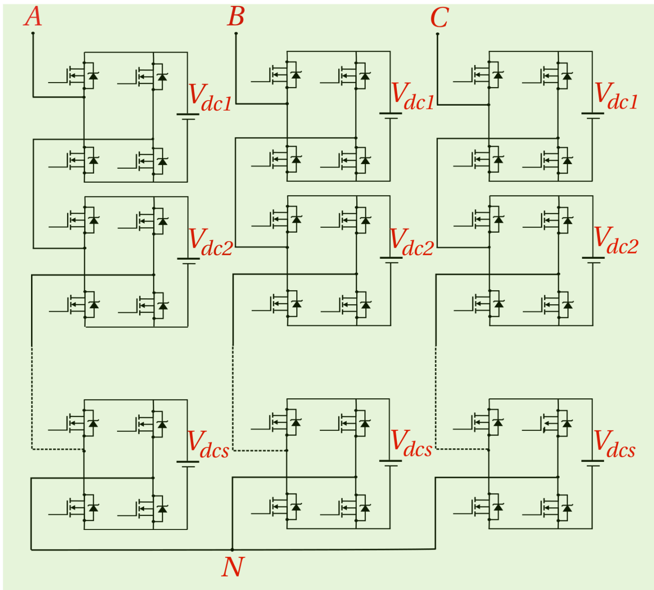

Figure 1: Three phase CHB l-level inverter.

A fundamental frequency SHE technique is proposed for three phase CHB l-level inverters having s H-bridges, as shown in Fig. 1. Considering for example the phase A, the Fourier series expansion of output phase voltage v_{AN} is

$$v_{AN}(\omega t) = \frac{4}{\pi} \sum_{k=1}^{\infty} \frac{1}{2k-1} H_{2k-1} \sin((2k-1)\omega t) \tag{1}$$

where

$$H_{2k-1} = \sum_{i=1}^{s} V_{dci} \cos((2k-1)\alpha_i) \tag{2}$$

The amplitude V_{2k-1} of the harmonic of order $(2k-1)$ can be expressed as

$$V_{2k-1} = \frac{4}{\pi(2k-1)} H_{2k-1} \tag{3}$$

The procedure assumes:

- fundamental switching frequency
- equispaced switching angles given by

$$\alpha_i = \alpha_1 + (i-1)\,\frac{\pi}{(l+r)} \quad i = 2,\,\ldots,\,s \tag{4}$$

where r is an integer parameter that can be assume the values $-2,\ -1,\ 0$ and $\alpha_1 = 0$ or $\alpha_1 = \frac{\pi}{2(l+r)}$

- unequal dc voltage sources $V_{dci},\ i = 1,\ldots,s$, expressed as

$$V_{dc1} = V_m \sin\left(\frac{\alpha_1 + \alpha_2}{2}\right) \tag{5}$$

$$V_{dci} = V_m \left[\sin\left(\frac{\alpha_i + \alpha_{i+1}}{2}\right) - \sin\left(\frac{\alpha_{i-1} + \alpha_i}{2}\right)\right] \tag{6}$$

$i = 2,\ldots,s-1$

$$V_{dcs} = V_m \left[\sin\left(\frac{\alpha_s + \vartheta}{2}\right) - \sin\left(\frac{\alpha_{s-1} + \alpha_s}{2}\right)\right] \tag{7}$$

where $\vartheta = \alpha_s + \pi/\,(l+r) = \alpha_1 + s\pi/\,(l+r)$ and V_m is assumed equal to $1\ p.u.$ for $m = 1$, as shown in Fig. 2.
If $\alpha_1 = 0$

$$V_{dc1} = V_m \sin\left(\frac{\pi}{2\,(l+r)}\right) \tag{8}$$

$$V_{dci} = V_m \left[\sin\left(\frac{(2i-1)\,\pi}{2\,(l+r)}\right) - \sin\left(\frac{(2i-3)\,\pi}{2\,(l+r)}\right)\right] \tag{9}$$

$i = 2,\ldots,s$
If $\alpha_1 \neq 0$

$$V_{dci} = V_m \left[\sin\left(\frac{i\pi}{l+r}\right) - \sin\left(\frac{(i-1)\,\pi}{l+r}\right)\right] \tag{10}$$

$i = 1,\ldots,s$
Fig. 2 shows the output phase voltage waveform of a three phase CHB 15-level inverter with $\alpha_1 = \frac{\pi}{30}$, $V_m = 1$ p. u., $r = 0$ and $\vartheta = \frac{\pi}{2}$.

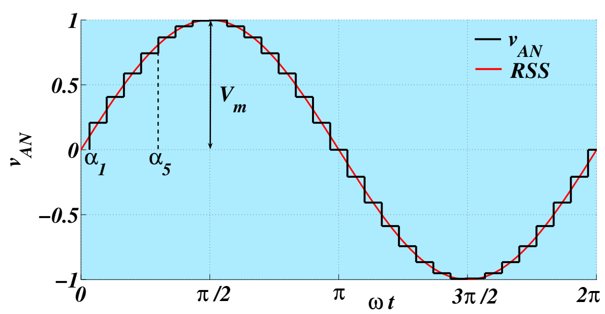

Figure 2: Output phase voltage waveform of a three phase CHB 15-level inverter with $\alpha_1 \neq 0$ and $r = 0$.

Depending on the parameter r and on the value of α_1 and considering a three phase CHB 15-level inverter, the obtained switching angles and the dc voltage sources for $m = 1$ are summarized in Table 1 and Table 2, respectively. In Figs. 3 and 4 the case with $\alpha_1 \neq 0$ is shown. It is observed that for $r = -2$ and $\alpha_1 \neq 0$ the value $V_{dc7} = 0$. $V_{dcs} = 0$ holds for each value of l.
Fig. 5 represents the case with $\alpha_1 = 0$, highlighting that V_{dc1} is lower respect to the other dc levels.

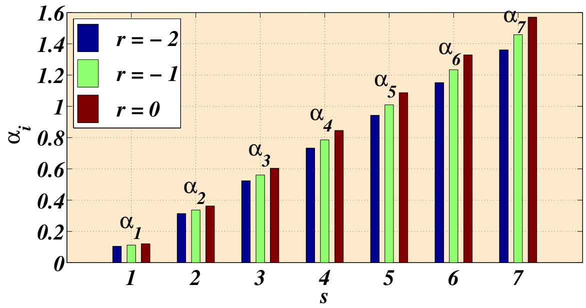

Figure 3: Switching angles depending on r with $\alpha_1 \neq 0$ for a three phase CHB 15-level inverter.

It is demonstrated in the next Section that, by applying the proposed procedure, the only undeleted harmonics are those of order $n = 2k\,(l+r) \pm 1,\ k = 1,\ 2,\ \ldots,\ r = -2,\ -1,\ 0$.

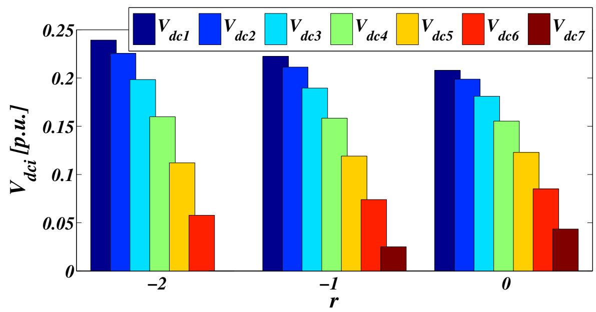

Figure 4: dc voltage sources depending on r with $\alpha_1 \neq 0$ for a three phase CHB 15-level inverter.

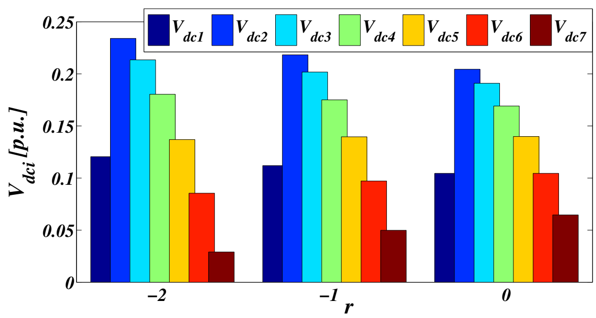

Figure 5: dc voltages sources depending on r with $\alpha_1 = 0$ for a three phase CHB 15-level inverter.

3. Mathematical proof

Assuming $n = 2k-1,\ k = 1,\ 2,\ \ldots,$ equation (2) becomes

$$H_n = \sum_{i=1}^{s} V_{dci} \cos\left(n\left(\alpha_1 + (i-1)\,\frac{\pi}{l+r}\right)\right) \tag{11}$$

The case considered for the proof is $\alpha_1 \neq 0$ and $r = -2,\ -1,\ 0$, therefore

$$H_n = V_m \sum_{i=1}^{s} \left[\sin\left(\tfrac{i\pi}{l+r}\right) - \sin\left(\tfrac{(i-1)\pi}{l+r}\right) \cdot \cos\left(\tfrac{(2i-1)\pi}{2(l+r)}\right)\right] \tag{12}$$

Table 1: **Switching angles (in [rad]) depending on the parameter r and on the value of α_1 for a three phase CHB 15-level inverter.**

r	α_1	$\alpha_i,\quad i=2,\cdots 7$	ϑ
-2	$\frac{\pi}{26}$	$\frac{3\pi}{26},\frac{5\pi}{26},\frac{7\pi}{26},\frac{9\pi}{26},\frac{11\pi}{26},\frac{13\pi}{26}$	$\frac{15\pi}{26}$
-2	0	$\frac{\pi}{13},\frac{2\pi}{13},\frac{3\pi}{13},\frac{4\pi}{13},\frac{5\pi}{13},\frac{6\pi}{13}$	$\frac{7\pi}{13}$
-1	$\frac{\pi}{28}$	$\frac{3\pi}{28},\frac{5\pi}{28},\frac{7\pi}{28},\frac{94\pi}{28},\frac{11\pi}{28},\frac{13\pi}{28}$	$\frac{15\pi}{28}$
-1	0	$\frac{\pi}{14},\frac{2\pi}{14},\frac{3\pi}{14},\frac{4\pi}{14},\frac{5\pi}{14},\frac{6\pi}{14}$	$\frac{\pi}{2}$
0	$\frac{\pi}{30}$	$\frac{3\pi}{30},\frac{5\pi}{30},\frac{7\pi}{30},\frac{9\pi}{30},\frac{11\pi}{30},\frac{13\pi}{30}$	$\frac{\pi}{2}$
0	0	$\frac{\pi}{15},\frac{2\pi}{15},\frac{3\pi}{15},\frac{4\pi}{15},\frac{5\pi}{15},\frac{6\pi}{15}$	$\frac{7\pi}{15}$

Table 2: **dc voltage sources depending on the parameter r and on the value of α_1 for a three phase CHB 15-level inverter for $m=1$.**

	V_{dci} [p.u.]					
r	**-2**	**-2**	**-1**	**-1**	**0**	**0**
α_1	$\frac{\pi}{26}$	0	$\frac{\pi}{28}$	**0**	$\frac{\pi}{30}$	**0**
V_{dc1}	0.239	0.121	0.223	0.112	0.208	0.105
V_{dc2}	0.225	0.234	0.211	0.218	0.199	0.204
V_{dc3}	0.198	0.213	0.190	0.202	0.181	0.191
V_{dc4}	0.160	0.180	0.158	0.175	0.155	0.169
V_{dc5}	0.112	0.137	0.119	0.140	0.123	0.140
V_{dc6}	0.058	0.085	0.074	0.097	0.085	0.105
V_{dc7}	0.0	0.029	0.025	0.050	0.043	0.065

Applying Prosthaphaeresis and Werner formulas, follows

$$H_n=2V_m\sin\left(\frac{\pi}{2(l+r)}\right)\cdot\sum_{i=1}^{s}\left[\cos\left(n\frac{(2i-1)\pi}{2(l+r)}\right)\cdot \cos\left(\frac{(2i-1)\pi}{2(l+r)}\right)\right] \tag{13}$$

and

$$H_n=V_m\sin\left(\frac{\pi}{2(l+r)}\right)\cdot\sum_{i=1}^{s}\left[\cos\left((n+1)\frac{(2i-1)\pi}{2(l+r)}\right)+ +(n-1)\cos\left(\frac{(2i-1)\pi}{2(l+r)}\right)\right] \tag{14}$$

Calling $S_q=\sum_{i=1}^{s}\cos\left(q\frac{(2i-1)\pi}{2(l+r)}\right)$ follows

$$H_n=V_m\sin\left(\frac{\pi}{2\,(l+r)}\right)(S_{n+1}+S_{n-1}) \tag{15}$$

The goal is to find the values of n such that $H_n=0$ and consequently $V_n=0$.
The following equality holds [29]

$$S_q=\sum_{i=1}^{s}\cos\left(q\frac{(2i-1)\pi}{2(l+r)}\right)= \tag{16}$$

$$\begin{cases}\frac{1}{2}\sin\left(\frac{\pi q(l-1)}{2(l+r)}\right)/\sin\left(\frac{\pi q}{2(l+r)}\right) & q\neq 2p\,(l+r)\,,\\ (-1)^p\,s & q=2p\,(l+r)\,,\ p=1,2,\ldots\end{cases}$$

If $q\neq 2p\,(l+r)\,,\ p=1,2,\ldots,q$ even, then

$$S_q=\frac{1}{2}\sin\left(\frac{\pi q\,(l-1)}{2\,(l+r)}\right)/\sin\left(\frac{\pi q}{2\,(l+r)}\right)= \tag{17}$$

$$\frac{1}{2}\sin\left(q\frac{\pi}{2}+q\frac{(-1-r)\,\pi}{2\,(l+r)}\right)/\sin\left(\frac{\pi q}{2\,(l+r)}\right)$$

therefore

$$S_q=\frac{1}{2}\cos\left(q\frac{\pi}{2}\right)\sin\left(q\frac{(-1-r)\,\pi}{2\,(l+r)}\right)/\sin\left(\frac{\pi q}{2\,(l+r)}\right)= \tag{18}$$

$$\begin{cases}0\ \ if\ \ r=-1\\ -\frac{1}{2}\cos\left(q\frac{\pi}{2}\right)=-\frac{1}{2}(-1)^{\frac{q}{2}}\ \ if\ \ r=0\\ \frac{1}{2}\cos\left(q\frac{\pi}{2}\right)=\frac{1}{2}(-1)^{\frac{q}{2}}\ \ if\ \ r=-2\end{cases}$$

Substituting $q=n\pm 1$, the quantity

$$(S_{n+1}+S_{n-1})= \tag{19}$$

$$\begin{cases}0\ \ if\ \ r=-1\\ \pm\frac{1}{2}\left[\cos\left((n+1)\,\frac{\pi}{2}\right)+\cos\left((n-1)\,\frac{\pi}{2}\right)\right]=\\ =\pm\frac{1}{2}\left[-\sin\left(n\frac{\pi}{2}\right)+\sin\left(n\frac{\pi}{2}\right)\right]=0\ \ if\ \ \ r=0,\,-2\end{cases}$$

If $q=2p\,(l+r)\,,\ p=1,2,\ldots$, and substituting $q=n\pm1$, then, for (16) and (18), follows

$$(S_{n+1}+S_{n-1})=\begin{cases}(-1)^p\,s\ \ if\ \ r=-1\\ (-1)^p\,s\pm\frac{1}{2}(-1)^{\frac{q}{2}}\ \ if\ \ r=0,\,-2\end{cases} \tag{20}$$

It is demonstrated that $H_n=0$ for $n\neq 2p\,(l+r)\pm 1$, $p=1,2,\ldots$, and consequently for (3) $V_n=0$.
Fig. 6 shows, for a three phase CHB 15-level inverter, the behavior of the quantity H_n for $V_m=1$ and $r=0$ as a

function of harmonic order n. It is possible to observe that H_n, represented in the graph as continuous function in n, is equal to zero for all odd n except $n = 30p \pm 1, \ p = 1, 2, \ldots$. For the case $\alpha_1 = 0$ the proof is similar.

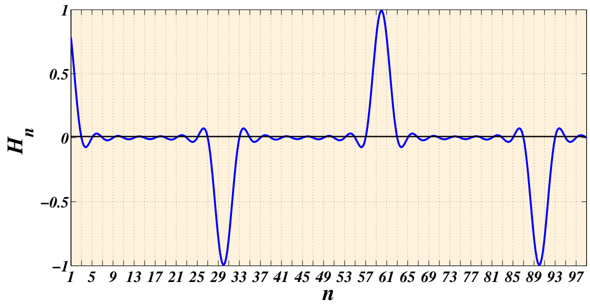

Figure 6: H_n for $\alpha_1 \neq 0$, $V_m = 1$ and $r = 0$.

4. Simulated results

This section reports some significant simulation results. THD%, chosen as a quality index, has been computed as

$$THD\% = \frac{\sqrt{\sum_{n=3,5,7,}^{131} V_n^2}}{V_1} \cdot 100 \tag{21}$$

Three phase CHB multilevel inverters are considered for the case $\alpha_1 \neq 0$ depending on parameter r.

Figs. 7, 8 and 9 show the weighed harmonics respect to the fundamental of the output phase voltage in a three phase CHB 15-level inverter, chosing $\alpha_1 = \frac{\pi}{2(15+r)}$ and $r = -2, -1, 0$, respectively. For each level, the case $\alpha_1 = 0$ gives similar results in terms of THD and harmonic analysis for $r = -2, -1$, but for $r = 0$ performs a harmonic mitigation as shown in Fig. 10.

Figs. 11, 12 and 13 show the harmonic analysis of the output phase voltage in a three phase CHB 29-level inverter for $r = -2$, $r = -1$ and $r = 0$, respectively. Considering up to the 131-th harmonic order, the last case returns the lower THD%, as confirmed in Fig. 14.

Fig. 14 shows THD% values of the output phase voltage in three phase CHB multilevel inverters, when the number of level l varies in the range $[5, 33]$. Since three phase topologies intrinsically delete the third and multiple harmonics, THD% presents discontinuous behavior at a given r and, depending on the level, the lower THD% is obtained for $r = -2$ or $r = -1$ or $r = 0$. The 29-level returns THD% less than 1% for $r = 0$. For $9, 15, 21, 27$ levels, $r = -1$ returns the lower THD%.

Considering $l = 5$ and $l = 7$, the THD% results obtained by the proposed technique are compared with those carried out by the classical SHE at the same conditions [20, 35]. Table 3 summarizes these results. It is possible to observe that the proposed modulation, for $r = 0$, returns lesser THD% values in the whole range of considered modulation index.

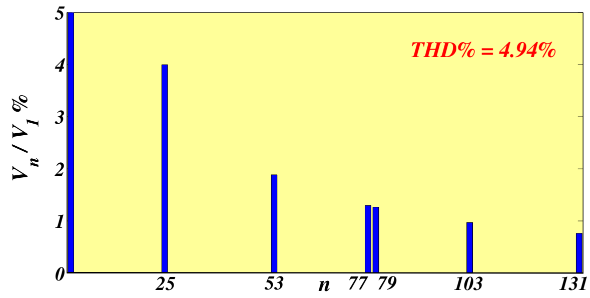

Figure 7: $V_n/V_1\%$ of output phase voltage in a three phase CHB 15-level inverter ($\alpha_1 \neq 0$, $r = -2$).

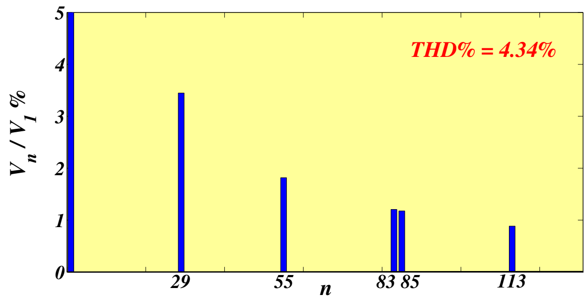

Figure 8: $V_n/V_1\%$ of output phase voltage in a three phase CHB 15-level inverter ($\alpha_1 \neq 0$, $r = -1$).

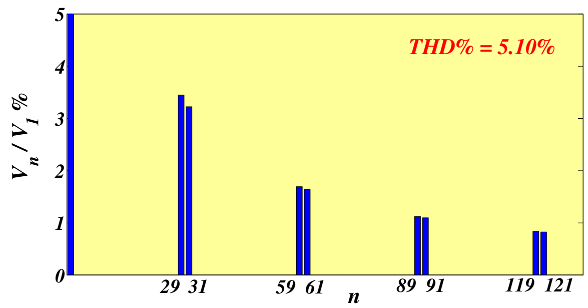

Figure 9: $V_n/V_1\%$ of output phase voltage in a three phase CHB 15-level inverter ($\alpha_1 \neq 0$, $r = 0$).

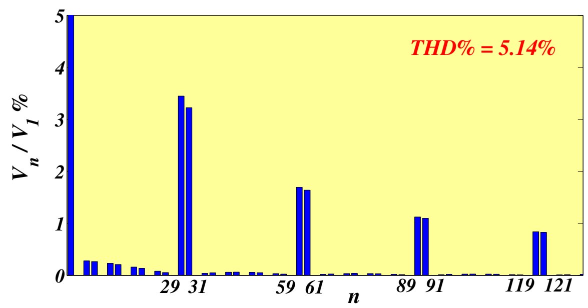

Figure 10: $V_n/V_1\%$ of output phase voltage in a three phase CHB 15-level inverter ($\alpha_1 = 0$, $r = 0$).

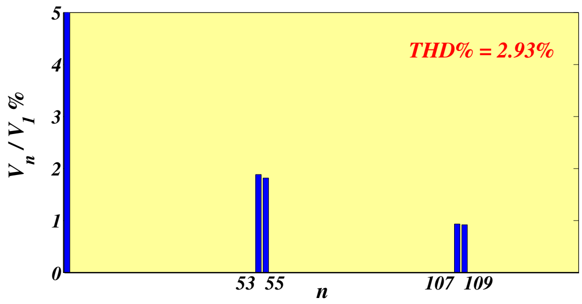

Figure 11: $V_n/V_1\%$ of output phase voltage in a three phase CHB 29-level inverter ($\alpha_1 \neq 0$, $r = -2$).

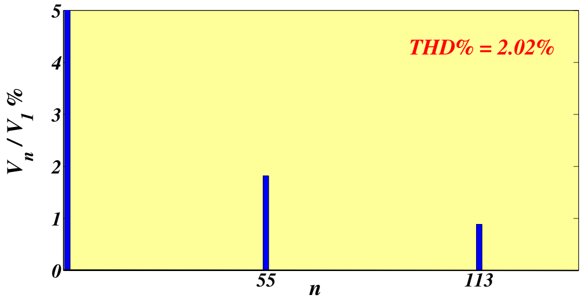

Figure 12: $V_n/V_1\%$ of output phase voltage in a three phase CHB 29-level inverter ($\alpha_1 \neq 0$, $r = -1$).

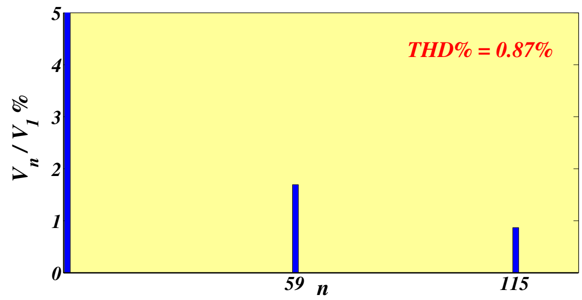

Figure 13: $V_n/V_1\%$ of output phase voltage in a three phase CHB 29-level inverter ($\alpha_1 \neq 0$, $r = 0$).

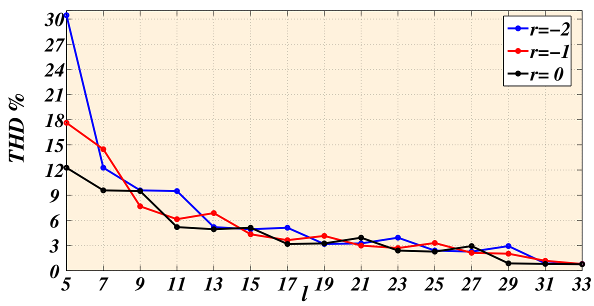

Figure 14: THD% of output phase voltage in a three phase CHB l-level inverter for $\alpha_1 \neq 0$.

5. Conclusions

In this paper a fundamental frequency SHE technique has been presented for three phase CHB l-level inverters. It requires variable dc sources, which is a drawback in industry and in smart grid applications, but not in renewable energy generation systems such as photovoltaic or wind generation systems in which the converter includes DC/DC stage. On the other side, proposed method eliminates a larger number of harmonics than conventional SHE, thus it allows to obtain low THD, that remains constant as the modulation index changes. Three different sets of switching angles have been defined for five and seven level inverters, by means of an integer parameter r, in the whole range of m. It has been demostrated through a mathematical proof and verified by simulation results that undeleted harmonics from output voltage waveform are only those of order $n = 2k\,(l + r) \pm 1$, $k = 1, 2, \ldots, r = -2, -1, 0$. The choice $r = 0$ has returned lower THD in comparison to the other r choices, except for $l = 9, 15, 21, 27$ where $r = -1$ represents the best choice. A three phase CHB 17-level inverter with $\alpha_1 = \frac{\pi}{34}$ and $r = 0$ returns THD% of about 3% and a 29-level with $\alpha_1 = \frac{\pi}{58}$ and $r = 0$ gives THD% less than 1%. Proposed modulation technique does not depend on the number of levels, and works at fundamental switching frequency, thus it offers low losses and consequently high efficiency. Ad additional advantage, is that it allows to satisfy grid code requirements using a lightweight and cheap filter.

References

[1] E. Hossain, J. Hossain, F. Un-Noor, "Utility Grid: Present Challenges and Their Potential Solutions," *IEEE Access*, vol. 6, pp. 60294-60317, 2018.

[2] A. Nasiri, A. Bani-Ahmed, I. Stamenkovic “Foundational Support Systems of the Smart Grid: State of the Art and Future Trends”, *Int. Journal of Smart Grid - ijSmartGrid*, vol. 2, no. 1, pp. 1-12, 2018.

[3] M. Caruso, R. Miceli, P. Romano, G. Schettino, F. Viola, “Technical and Economical Performances of Photovoltaic Generation Façades,” *Int. Journal of Smart Grid - ijSmartGrid*, vol. 2, no. 2, pp. 87-98, 2018.

[4] H. Abu-Rub, J. Holtz, J. Rodriguez, G. Baoming, “Medium-voltage multilevel converters-State of the art, challenges, and requirements in industrial applications,” *IEEE Trans. Ind. Electron.*, vol. 57, no. 8, pp. 2581–2596, Aug. 2010.

[5] M. Roknuzzaman, S. Hamasaki, “Control of Full Bridge Type Modular Multilevel Converter for AC/AC Conversion with Grid Connection,” *Int. Conf. on Smart Grids (icSmartGrids),* Nagasaki Prefectural Art Museum, Nagasaki, Japan, Dec. 4-6, 2018.

[6] L. Comparatore, A. Renault, J. Pacher, Jorge Rodas, René Gregor, “Finite Control Set Model Predictive

Table 3: **THD% comparisons.**

THD% for $l = 5$

m	**Proposed technique** $r = 0$ $\left(\frac{\pi}{10}, \frac{3\pi}{10}\right)$	$r = -1$ $\left(\frac{\pi}{8}, \frac{3\pi}{8}\right)$	$r = -2$ $\left(\frac{\pi}{6}, \frac{3\pi}{6}\right)$	**SHE [20]**
0.85	12.27	17.63	30.45	17.80
0.80	12.27	17.63	30.45	20.43
0.75	12.27	17.63	30.45	30.45
0.70	12.27	17.63	30.45	29.32
0.65	12.27	17.63	30.45	29.66
0.60	12.27	17.63	30.45	30.74
0.55	12.27	17.63	30.45	31.95
0.50	12.27	17.63	30.45	32.51

(a) THD% obtained by the proposed technique and by the standard SHE [20] for three phase CHB 5-level inverter.

THD% for $l = 7$

m	**Proposed technique** $r = 0$ $\left(\frac{\pi}{14}, \frac{3\pi}{14}, \frac{5\pi}{14}\right)$	$r = -1$ $\left(\frac{\pi}{12}, \frac{3\pi}{12}, \frac{5\pi}{12}\right)$	$r = -2$ $\left(\frac{\pi}{10}, \frac{3\pi}{10}, \frac{5\pi}{10}\right)$	**SHE [35]**
0.84	9.57	14.48	12.27	15.83
0.80	9.57	14.48	12.27	11.06
0.75	9.57	14.48	12.27	11.87
0.70	9.57	14.48	12.27	16.43
0.65	9.57	14.48	12.27	15.95
0.60	9.57	14.48	12.27	12.49
0.55	9.57	14.48	12.27	14.16
0.50	9.57	14.48	12.27	12.21

(b) THD% obtained by the proposed technique and by the standard SHE [35] for three phase CHB 7-level inverter.

Control Strategies for a Three-Phase Seven-level Cascade H-Bridge DSTATCOM," 7th *Int. Conf. on Renewable Energy Research and Applications, (ICRERA)*, Paris, France, 2018.

[7] R. Teodorescu, F. Blaabjerg, J. K. Pedersen, E. Cengelci, and P. N. Enjeti, "Multilevel inverter by cascading industrial VSI," *IEEE Trans. Ind. Electron.*, vol. 49, no. 4, pp. 832–838, Aug. 2002.

[8] K. K. Gupta and S. Jain, "A novel multilevel inverter based on switched DC sources," *IEEE Trans. Ind. Electron.*, vol. 61, no. 7, pp. 3269–3278, July 2014.

[9] A. K. Rathore, J. Holtz, T. Boller, "Generalized optimal pulsewidth modulation of multilevel inverters for low-switching-frequency control of medium-voltage high-power industrial AC drives," *IEEE Trans. Ind. Electron.*, vol. 60, no. 10, pp. 4215–4224, Oct. 2013.

[10] F. Viola, V. Castiglia, G. Schettino, C. Cecati, C. Buccella, M. Cimoroni, R. Miceli, "Mixed Harmonic Elimination Control for a Single-Phase 9-Level Grid-Connected Inverter" *Int. Conf. on Smart Grids (icSmartGrids)*, Nagasaki Prefectural Art Museum, Nagasaki, Japan, Dec. 4-6, 2018.

[11] E. Babaei and S. H. Hosseini, "New cascaded multilevel inverter topology with minimum of switches," *Energy Convers. and Manag.*, vol. 50, no. 4, pp. 2761–2767, 2009.

[12] R. S. Alishah, D. Nazarpour, S. Hosseini, M. Sabahi, "Novel topologies for symmetric, asymmetric, and cascade switched-diode mutilevel converter with minimum number of power electronic components," *IEEE Trans. Ind. Electron.*, vol. 61, no. 10, pp. 5300–5310, Oct. 2014.

[13] R. S. Alishah and D. Nazarpour, "New hybrid structure for multilevel inverter with fewer number of components for high-voltage levels," *IET Power Electron.*, vol. 7, no. 1, pp. 96–104, 2013.

[14] C. Buccella, C. Cecati, M. G. Cimoroni, "Performance analysis and simulation of unbalanced DC sources five level inverter topology," *4th Int. Conf. on Renewable Energy Research and Applications, (ICRERA)*, Palermo, Italy, 22-25 Nov. 2015.

[15] E. Babaei, S. H. Hosseini, G. B. Gharehpetian, M. T. Haque, M. Sabahi, "Reduction of dc voltage sources and switches in asymmetrical multilevel converters using a novel topology," *Elect. Power Syst. Res.*, vol. 77, no. 8, pp. 1073–1085, 2007.

[16] B. P. McGrath and D. G. Holmes, "Multicarrier PWM strategies for multilevel inverters," *IEEE Trans. Ind. Electron.*, vol. 49, no. 4, pp. 858–867, Aug. 2002.

[17] B. N. Roodsari and E. P. Nowicki, "Fast space vector modulation algorithm for multilevel inverters and its extension for operation of the cascaded H-bridge inverter with non-constant DC sources," *IET Power Electron.*, vol. 6, no. 7, pp. 1288–1298, 2013.

[18] H. Benbouhenni, "Comparative Study Between Direct Vector Control and Fuzzy Sliding Mode Controller in Three-Level Space Vector Modulation Inverter of Reactive and Active Power Command of DFIG-Based Wind Turbine Systems," *Int. Journal of Smart Grid - ijSmartGrid*, vol. 2, no. 4, pp. 188-196, 2018.

[19] C. Buccella, C. Cecati, M. G. Cimoroni, K. Razi, "Analytical method for pattern generation in five-level cascaded H-bridge inverter using selective harmonic elimination," *IEEE Trans. Ind. Electron.,* vol. 61, no. 11, pp. 5811-5819, Nov. 2014.

[20] C. Buccella, C. Cecati, M. G. Cimoroni, G. Kulothungan, A. Edpuganti, A. Kumar Rathore, "A Selective Harmonic Elimination Method for Five-Level Converters for Distributed Generation," *IEEE Journal of Emerg. and Select. topic in Pow. Elec.,* vol. 5, no. 2, pp. 775-783, June 2017.

[21] A. Shukla, A. Ghosh, A. Joshi, "Hysteresis modulation of multilevel inverters," *IEEE Trans. Power Electron.*, vol. 26, no. 5, pp. 1396–1409, May 2011.

[22] S. Gautam and R. Gupta, "Switching frequency derivation for the cascaded multilevel inverter operating in current control mode using multiband hysteresis modulation," *IEEE Trans. Power Electron.*, vol. 29, no. 3, pp. 1480–1489, Mar. 2014.

[23] R. Gupta, A. Ghosh, A. Joshi, "Multiband hysteresis modulation and switching characterization for sliding mode controlled cascaded multilevel inverter," *IEEE Trans. Ind. Electron.*, vol. 57, no. 7, pp. 2344–2353, Jul. 2010.

[24] S. Moulahoum, M. Hallouz, N. Kabache, S. Kouadria, "Neural Network Based Field Oriented Control for Doubly-Fed Induction Generator," *Int. Journal of Smart Grid - ijSmartGrid*, vol. 2, no. 3, pp. 183-187, 2018.

[25] G. Niyitegeka, E. M. Harerimana, G. Park, J. Choi, "Phase Shift Modulation and Dc-Link's Voltage Balancing Control for a Dab DC-DC Converter," *Int. Conf. on Smart Grids (icSmartGrids),* Nagasaki Prefectural Art Museum, Nagasaki, Japan, Dec. 4-6, 2018.

[26] S. Kannan, P. Mekala, I. Colak , W. Ali, "Selective Harmonic Elimination for Modular Multilevel Converter with Averaging and Circulating Current Control," 7th *Int. Conf. on Renewable Energy Research and Applications, (ICRERA)*, Paris, France, 2018.

[27] M. Sharifzadeh, H. Vahedi, C. Cecati, C. Buccella, K. Al-Haddad, "A generalized formulation of SHM-PAM for cascaded H-bridge inverters with non-equal DC sources," *IEEE Int. Conf. on Ind. Technology (ICIT17)*, pp. 18-23, Toronto, Canada, March 22-25, 2017.

[28] P. L. Kamani and M.A. Mulla, "Middle-level SHE Pulse-Amplitude Modulation for Cascaded Multilevel Inverters," *IEEE Trans. Ind. Electron.,* vol. 65, no. 3, pp. 2828-2833, March 2018.

[29] C. Buccella, M.G. Cimoroni, M. Tinari, C. Cecati, "A new pulse active width modulation (PAWM) for multilevel converters," *IEEE Trans. Power Electron.*, 2019, (Early Access).

[30] M. G. Cimoroni, M. Tinari, C. Buccella, C. Cecati, "A high efficiency Selective Harmonic Elimination technique for multilevel converters," *2018 Int. Symp. on Power Electron. Electrical Drives, Automation and Motion (SPEEDAM)*, Amalfi, Italy, pp. 673-677, 20-22 June, 2018.

[31] A. Perrez-Basante, S. Ceballos, G. Konstantinou, J. Pou, I. Kortabarria, I. M. de Alegria, "A universal formulation for multilevel selective-harmonic-eliminated PWM with half-wave symmetry," *IEEE Transactions on Power Electron.,* vol. 34, no. 1, pp. 943–957, Jan 2019.

[32] M. H. Etesami, D. M. Vilathgamuwa, N. Ghasemi, D. P. Jovanovic, "Enhanced metaheuristic methods for selective harmonic elimination technique," *IEEE Trans. on Ind. Inf*., vol. 14, no. 12, pp. 5210–5220, Dec. 2018.

[33] K. Yang, M. Feng, Y. Wang, X. Lan, J. Wang, D. Zhu, W. Yu, "Real-time switching angles computation for selective harmonic control," *IEEE Trans. on Power Electron.*, 2019, (Early Access).

[34] S. Kundu, A. D. Burman, S. K. Giri, S. Mukherjee, S. Banerjee, "Comparative study between different optimisation techniques for finding precise switching angle for SHE-PWM of three-phase seven-level cascaded h-bridge inverter," *IET Power Electron.*, vol. 11, no. 3, pp. 600–609, 2018.

[35] C. Buccella, M. G. Cimoroni, H. Latafat, G. Graditi, R. Yang, "Selective harmonic elimination in a seven level cascaded multilevel inverter based on graphical analysis," *IEEE Int. Conf. on Ind. Electron. (IECON16)*, pp. 2563–2568, Florence, Italy, Oct. 24-27, 2016.